frontiers | Frontiers in Cellular and Infection Microbiology

TYPE Original Research
PUBLISHED 14 May 2024
DOI 10.3389/fcimb.2024.1384611

OPEN ACCESS

EDITED BY
Isaura Simões,
Old Dominion University, United States

REVIEWED BY
Lee-Ann H. Allen,
University of Missouri, United States
Ann Jerse,
Uniformed Services University, United States

*CORRESPONDENCE
Ana-Maria Dragoi
anamaria.dragoi@lsuhs.edu

RECEIVED 09 February 2024
ACCEPTED 23 April 2024
PUBLISHED 14 May 2024

CITATION
Juárez Rodríguez MD, Marquette M, Youngblood R, Dhungel N, Torres Escobar A, Ivanov SS and Dragoi A-M (2024) Characterization of *Neisseria gonorrhoeae* colonization of macrophages under distinct polarization states and nutrients environment. *Front. Cell. Infect. Microbiol.* 14:1384611. doi: 10.3389/fcimb.2024.1384611

Characterization of *Neisseria gonorrhoeae* colonization of macrophages under distinct polarization states and nutrients environment

María Dolores Juárez Rodríguez[1], Madison Marquette[2], Reneau Youngblood[1], Nilu Dhungel[1], Ascención Torres Escobar[3], Stanimir S. Ivanov[3] and Ana-Maria Dragoi[1,4]*

[1]Department of Molecular and Cellular Physiology, LSUHSC-Shreveport, Louisiana, LA, United States, [2]LSU Health Shreveport, School of Medicine, Louisiana, LA, United States, [3]Department of Microbiology and Immunology, LSUHSC-Shreveport, Louisiana, LA, United States, [4]Feist-Weiller Cancer Center, LSUHSC-Shreveport, Louisiana, LA, United States

Neisseria gonorrhoeae (Ng) is a uniquely adapted human pathogen and the etiological agent of gonorrhea, a sexually transmitted disease. *Ng* has developed numerous mechanisms to avoid and actively suppress innate and adaptive immune responses. *Ng* successfully colonizes and establishes topologically distinct colonies in human macrophages and avoids phagocytic killing. During colonization, *Ng* manipulates the actin cytoskeleton to invade and create an intracellular niche supportive of bacterial replication. The cellular reservoir(s) supporting bacterial replication and persistence in gonorrhea infections are poorly defined. The manner in which gonococci colonize macrophages points to this innate immune phagocyte as a strong candidate for a cellular niche during natural infection. Here we investigate whether nutrients availability and immunological polarization alter macrophage colonization by *Ng*. Differentiation of macrophages in pro-inflammatory (M1-like) and tolerogenic (M2-like) phenotypes prior to infection reveals that *Ng* can invade macrophages in all activation states, albeit with lower efficiency in M1-like macrophages. These results suggest that during natural infection, bacteria could invade and grow within macrophages regardless of the nutrients availability and the macrophage immune activation status.

KEYWORDS

***Neisseria gonorrhoeae*, macrophage colonization, macrophage polarization, immune evasion, bacteria invasion, intracellular growth**

Introduction

Gonorrhea, a sexually transmitted infection (STI) caused by the obligate human pathogen *Neisseria gonorrhoeae* (*Ng*) is rising worldwide with > 80 million new cases annually (Unemo et al., 2016; Unemo et al., 2021). *Ng* mainly colonizes and infects the urogenital tract (Quillin and Seifert, 2018). In men, gonorrhea mostly manifests as symptomatic urethritis, while in women the infection can remain asymptomatic making detection and early treatment difficult. A significant number of women (15%) develop ascending pelvic inflammatory disease with serious complications including chronic pelvic pain, infertility, increased risk of ectopic pregnancy, and endometriosis (McGee et al., 1981; Lenz and Dillard, 2018; Stevens and Criss, 2018). One clinical problem is the widespread rapid emergence of multi-drug resistant strains, which limits therapeutic options. In 2019, CDC classified drug-resistant *Ng* as an urgent threat. Another significant challenge is vaccine development, due to the diverse immune evasion mechanisms utilized by *Ng* to avoid killing and suppress immunological responses (Rice et al., 2017; Quillin and Seifert, 2018).

The localized innate immune response at the sites of bacterial colonization drives the immuno-pathology central to gonorrhea disease (Hook, 1987; Givan et al., 1997; Quillin and Seifert, 2018). Macrophages and neutrophils are key players in mucosal immune defenses (Dwivedy and Aich, 2011). In symptomatic gonorrhea, monitoring exudate secretions for neutrophils harboring gonococci is a classical early diagnostic test (Quillin and Seifert, 2018). Thus, historically, neutrophils have been the research focus (Dilworth et al., 1975; Criss and Seifert, 2008; Criss et al., 2009; Criss and Seifert, 2012; Gunderson and Seifert, 2015; Palmer and Criss, 2018) and many aspects of *Ng* interaction with neutrophils have been elucidated, including the observation that neutrophils can support limited bacterial replication *ex vivo* (Palmer and Criss, 2018). New data, however, demonstrated that macrophages have a high capacity to support *Ng* replication (>2–3 orders of magnitude in 8hrs) in nutrient-depleted environments for >24 hrs (Chateau and Seifert, 2016; Ivanov et al., 2021). Exudate secretions in acute gonorrhea besides neutrophils and exfoliated epithelial cells also contain macrophages (Hook, 1987). Furthermore, macrophages are present throughout the genitourinary mucosa, representing about 10% of all mucosa-resident leukocytes (Givan et al., 1997; Pudney et al., 2005), and are recruited to and infiltrate the uterine mucosa in murine models of vaginal gonorrhea (Imarai et al., 2008; Song et al., 2008). Thus, macrophages could be one cellular niche for *Ng* replication and persistence in human infections. Indeed, we showed that *Ng* can colonize and invade macrophages forming both surface-associated as well as intracellular colonies (Ivanov et al., 2021). The invasion process is carried out by a novel mechanism via FMNL3-regulated actin-dependent membrane morphogenesis, which was observed for both human differentiated U937 macrophages as well as primary human monocyte-derived macrophages (hMDMs). Additionally, gonococci can inhibit apoptosis in human macrophages, and have been shown to elicit secretion of both inflammatory and tolerogenic cytokines by macrophages (Escobar et al., 2013; Chateau and Seifert, 2016; Escobar et al., 2018). The emerging data argue for further investigation of macrophages as a cellular niche and regulators of immunological responses in gonorrhea.

Ng colonizes macrophages in a manner that facilitates immune evasion. We have shown that an early step in invasion is the establishment of a surface microcolony, which entails attachment, inhibition of canonical phagocytosis, and bacterial replication on the surface of the host cell (Ivanov et al., 2021). Some colonies remain surface-associated, while others trigger membrane remodeling and the formation of an invasion platform where the actin nucleating factor FMNL3 is recruited and promotes actin polymerization and colony uptake (Ivanov et al., 2021). During invasion, the colony stretches from the surface of the host cell into a plasma membrane-derived membrane-bound compartment that cradles a fraction of the colony. The simultaneous existence of surface-associate, intracellular, and partially internalized hybrid bacterial colonies would benefit immune evasion. This adaptation to multiple topologically distinct niches is a complex evolutionary solution counteracting multiple distinct host defense responses. A surface-associated niche protects *Ng* from several cell-autonomous defense responses against intracellular pathogens (such as lysosomal degradation, autophagy, and host cell death) (Bah and Vergne, 2017; Jorgensen et al., 2017; Krakauer, 2019), whereas an intracellular niche safeguards against humoral defenses targeting extracellular bacteria (such as complement, circulating antibodies, and anti-microbial peptides) (Dunkelberger and Song, 2010). Indeed, when macrophages invasion was blocked by cytochalasin D or in FMNL3-depleted cells, the number of bacteria protected from antibiotic killing decreased by ~70% as determined by CFU assays (Ivanov et al., 2021). Thus, the FMNL3-mediated gonococcal internalization by human macrophages protects gonococci from extracellular microbiocidal activities.

The impact of nutrients availability and macrophage immune polarization on gonococci capacity to colonize, invade, and replicate within human macrophages is investigated here. The extracellular micronutrients in the urogenital mucosa vary based on gender (Nelson et al., 2010; Dong et al., 2011; Tuddenham et al., 2019; Barrientos-Durán et al., 2020) and over time during the reproductive cycle in women (Grobeisen-Duque et al., 2023). Thus, it is important to establish whether nutrients limitation impacts macrophage colonization and invasion by gonococci. In addition, macrophages can undergo phenotypic polarization in response to the environmental cues to carry out tissue surveillance and homeostasis functions (Locati et al., 2020; Nobs and Kopf, 2021). The distinct polarization states can impact macrophage-driven immunological responses to infection (Sica and Mantovani, 2012; Atri et al., 2018; Almeida et al., 2023). The classically activated M1 macrophages have enhanced microbiocidal capacity, secrete pro-inflammatory/T helper 1 (Th1)-promoting cytokines (IL-12, IL-1β, IL-6, and TNF-α), and mediate host defense against bacterial, viral and protozoal pathogens (Atri et al., 2018). The alternatively activated M2 macrophages mediate tissue repair and exhibit a more tolerogenic immunological profile by preferential secretion of anti-inflammatory mediators (IL-10 and

TGF-β) (Martinez et al., 2009). Polarization towards the M1 state can be elicited by stimulation with IFN-γ and lipopolysaccharide (LPS), while M2 polarization is triggered by stimulation with IL-4, IL-10, and IL-13 (Shapouri-Moghaddam et al., 2018). Because gonococci are likely to encounter macrophages in distinct polarization states in symptomatic *vs.* asymptomatic infections, it is important to determine the impact on colonization and invasion.

Materials and methods

Bacterial strains and culture conditions

Neisseria gonorrhoeae FA1090, was a gift from Dr. Hank Seifert (Northwestern University). FA1090-LuxR strain was generated as detailed below. Bacteria were cultured on gonococcal medium base (GCB) agar (Criterion) with Kellogg's supplements (Kellogg et al., 1963) at 37°C and 5% CO_2 for approximately 16 hrs. For infections, 4 to 6 piliated Opa+ colonies as determined by colony morphology were pooled, streaked on GCB agar (1x1cm patch) and grown for another 16 hrs. Patches were collected and resuspended in PBSG (PBS supplemented with 7.5 mM Glucose, 0.9 mM $CaCl_2$, and 0.7 mM $MgCl_2$). The number of bacteria was determined by OD_{600} measurements. Inocula for infections were prepared in PBSG, RPMI or RPMI containing inactivated human serum (10%) and the number of bacteria was confirmed by plating dilutions from the inoculum on GCB agar. *Legionella pneumophila* serogroup 1 strain JR32 Δ*flaA luxR* was used in this study (Ondari et al., 2023). The *Legionella* strain was grown on charcoal yeast extract (CYE) plates composed of 1% yeast extract, 1%N-(2-acetamido)-2-aminoethanesulphonic acid (ACES; pH 6.9), 3.3 mM l-cysteine, 0.33 mM $Fe(NO3)_3$, 1.5% agar, 0.2% activated charcoal (Feeley et al., 1979). For macrophage infections *Legionella* was obtained from day 2 heavy patches grown on CYE plates and was resuspended to OD_{600} of 0.5 U in 1 ml AYE, placed in 15-ml glass culture tubes, and cultivated aerobically 24 to 26 hrs with continuous shaking (175 rpm) at 37°C until early stationary phase was reached (OD_{600} range of 2.0 to 3.0 U). For propagation and plating of *Escherichia coli*, Luria-Bertani (LB) broth and LB agar (LB broth with 1.5% agar) were used. As needed, the culture media were supplemented with 2 μg/ml erythromycin.

Construction of the plasmid pMR32-MCS-*luxCDABE*

The construction of the plasmid pMR32-MCS-*luxCDABE* for the generation of *Neisseria gonorrhoeae* FA1090-LuxR luminescent strain was performed in two steps: (1) A 95-bp DNA fragment containing a multi-cloning site flanked by cohesive ends for PmeI and ApaI restriction enzymes, was generated by the annealing of the following primers:

pMR32MCS_F_(5′AAACTCACTAGTCATGTC GACTTCGAATTCGTCCATTCCTGCAGGTCTGA GCTCTATCCTAGGATGCCGTCCGAACCTTCAGAC GGCATTGGGCC 3′)

pMR32MCS_R::(5′CAATGCCGTCTGAAGGTTCGGACGG CATCCTAGGATAGAGCTCAGACCTGCAGGAATGG ACGAATTCGAAGTCGACATGACTAGTGAGTTT 3′).

The resulting DNA product was phosphorylated and cloned into the pMR32 plasmid (Ramsey et al., 2012) digested with PmeI and ApaI to obtain the pMR32-MCS plasmid. (2) The *Photorharddus luminescens luxCDABE* operon was PCR amplified using as a template the pXen-13 plasmid (Xenogen Bioware) with the following primer set:

lux_F (5′ TATGGGGAAGTCGACTTGGAGGATACGTA TGACTAAAAAAATTTC 3′)

lux_R (5′ GAATTAACGAGCTCGAATACCTGCAGGTC ATCAACTATCAAAC 3′)

The 5857-bp amplicon was digested with SalI and SacI and cloned into the pMR32-MCS plasmid digested with the same enzymes to generate the pMR32-MCS-*luxCDABE* plasmid that harbors the *Photorharddus luminescens luxCDABE* operon under the control of *Neisseria gonorrhoeae opaB* promoter.

Generation of *Neisseria gonorrhoeae* FA1090-LuxR luminescent strain

Neisseria gonorrhoeae FA1090 was grown from frozen stocks onto the GCB agar (Criterion) with 1% Kellogg's supplements at 37°C and 5% CO_2 for 16 hrs. From bacteria grown on GCB agar, 5 piliated colonies were collected and pooled in GC Broth (1.5% Difco proteose peptone no. 3, 0.4% K_2HPO_4, 0.1% KH_2PO_4, 0.1% NaCl, pH of 7.2, with 1% Kellogg's supplements and 0.042% $NaHCO_3$), and were naturally transformed with 1 μg of pMR32-MCS-*luxCDABE* plasmid DNA onto GCB agar. The plate was incubated at 37°C with 5% CO_2, for 16 h. The next day, the bacteria were harvested from the plate, resuspended in GC Broth, seeded onto GCB agar plates containing 2μg/ml erythromycin, and incubated at 37°C with 5% CO_2, for 16h. The erythromycin-resistant colonies were collected and analyzed by PCR amplification with the following primer set:

F_ermC (5′- GAACATGATAATATCTTTGAAATCGGC TCAG -3′)

R_ermC (5′ -CTTGTATTCTTTGTTAACCCATTTCATAAC G-3′).

The allelic exchange was confirmed in individual colonies by kanamycin sensitivity, erythromycin resistance, PCR amplification of the 525-bp fragment, and bioluminescence.

Ratio of CFUs to bioluminescence calculation

Neisseria gonorrhoeae FA1090-LuxR strain was grown on GCB agar plates supplemented with Erythromycin at 2 μg/ml, harvested

in GC Broth, and resuspended at an OD_{600} = 0.5 U in GC broth. Then, 2-fold serial dilutions were made in the same medium and 200 µl aliquots of each dilution were distributed in triplicate in a white-wall clear bottom 96-well assay plate (Corning). The OD_{600} and luminescence data were acquired in a luminescence plate reader (BioTek Synergy H1, Agilent). The number of bacterial colony-forming units (CFUs) was determined by plating serial dilutions from which bioluminescence light output per OD_{600} unit or per CFU was calculated.

Axenic growth kinetics of *Neisseria gonorrhoeae* strains

Bacteria grown on GCB agar were harvested and resuspended at an OD_{600} = 0.5 U in GC Broth. Then, 2-fold serial dilutions were made until at an OD_{600} = 0.0078 U in the same medium. Next, 200 µl of selected 2-fold dilutions were distributed by sextuplicate in a white-wall clear bottom 96-well assay plate (Corning). The plate was incubated in a luminescence plate reader (BioTek Synergy H1, Agilent) at 37°C for 24 hrs. The OD_{600} and luminescence data were automatically collected every 10 minutes after the cultures were agitated for 15 sec (double orbital rotation, 150 rpm). Bioluminescence output from each well was acquired for one second and presented as total relative light unit (RLU) counts/s.

Neisseria gonorrhoeae axenic growth kinetics under different nutrient conditions

The bacteria were grown on GCB agar and harvested in PBSG (PBS supplemented with 7.5 mM Glucose, 0.9 mM $CaCl_2$, and 0.7 mM $MgCl_2$). Then, the bacteria were resuspended at an OD_{600} = 0.5 U in three different nutritional culture conditions: (i) PBSG containing 25 mM HEPES (HyClone GE Healthcare Life Sciences), (ii) RPMI medium (Genesee) with 25 mM HEPES and (iii) RPMI with 25 mM HEPES and supplemented with 10% heat-inactivated human serum (Sigma-H4522). Then, 2-fold serial dilutions were made in each medium and 200 µl of selected 2-fold dilutions were distributed by sextuplicate in a white-wall clear bottom 96-well assay plate (Corning). The plate was incubated in the luminescence plate reader at 37°C for 24 hrs and OD_{600} and bioluminescence were acquired as described above.

Neisseria gonorrhoeae inoculum preparation

For infection of macrophages, bacterial strains were grown from frozen stocks onto GCB agar for 16 hrs. The next day, 5 piliated colonies were pooled and streaked on GCB and were grown for another 16 hrs. On the second day, bacteria were collected and resuspended in PBSG. Bacterial numbers were determined by OD_{600} measurements. The inoculum was prepared at MOI = 5 in the media used in the infection assay. Inocula for all infections were confirmed by plating dilutions on GCB agar for CFU recovery.

Cell culture conditions

The human monocytic cell line U937 (ATCC CRL-1593.2) was obtained from ATCC and primary human peripheral monocytic cells (PBMCs) were purchased from Sigma (HUMANPBMC-0002644). U937 cells were cultured in RPMI medium (Genesee) supplemented with 10% Fetal Bovine Serum (FBS) at 37°C and 5% CO_2. For differentiation into mature adherent macrophages, U937 monocytes were seeded at the desired density, cultured with 10 ng/ml phorbol 12-myristate 13-acetate (PMA) for 24 hrs, followed by 48 hrs incubation with RPMI media (+10% FBS) (v/v) in the absence of PMA. For M1 and M2 polarization, U937 cells differentiated with PMA, were treated with 25 ng/ml IFNγ (BioLegend catalog #713906) and 100 ng/ml *Escherichia coli* lipopolysaccharides (LPS) for 24 hrs to induce M1 polarization or 25 ng/ml IL-4 (BioLegend catalog #766202) and 25 ng/ml IL-13 (BioLegend catalog #571102) for M2 polarization. Primary human PBMC were differentiated into macrophages (hMDMs) after culturing for 7 days with RPMI supplemented with 20% heat-inactivated human serum (Sigma-H4522).

Quantitative analysis of bacterial replication in infection assays

Cells were seeded at $5x10^4$ cells per well in a white-wall clear bottom 96-well assay plate (Corning 3610) for infection assays. U937 monocytes were directly differentiated in 96-well plates, whereas hMDMs were differentiated first and then seeded in the plates for infection. For infection of polarized macrophages, cells cultured in RPMI (+10% FBS) (v/v) were treated with the respective cytokines (as detailed above) for 24 hrs prior to the infection. The media were replaced with either PBSG, RPMI, or RPMI supplemented with 10% heat-inactivated human serum for the infection assays. All media were supplemented with 25 mM HEPES. For both *Neisseria* and *Legionella*, macrophages were infected at MOI = 5 and infections were carried out in six technical replicates for every condition. The 96-well plates were incubated in the luminescence plate reader at 37°C for 24 hrs (for *Ng*) or 72 hrs (for *Lp*) and bioluminescence output was obtained hourly. Light was collected for 1s per well and the data is presented as total relative light unit (RLU) counts/s.

Microscopy analyses of infected cells

U937 monocytes seeded at $2x10^5$ cells/well were differentiated into macrophages directly on coverslips in 24-well plates (Gen Clone). Macrophages were polarized as detailed above and infected with *Ng* FA1090 strain (MOI = 5) in the indicated media for 8 hrs. To stop the infection, the coverslips were washed three times with warm PBS and fixed with 4% paraformaldehyde (PFA) (Electron Microscopy Sciences) at 4°C overnight. Subsequently, coverslips were blocked with 2% goat serum in PBS for 30 min, and an anti-*Ng* chicken IgY antibody (diluted 1:100 in PBS) was added for 1 hour at ambient temperature for detection of extracellular bacteria. Next, the coverslips were washed 3X with PBS, fixed with 4% PFA for 30min, washed 3X with PBS, permeabilized and blocked

simultaneously with 0.1% TritonX-100 and 2% goat serum in PBS for 60 min at ambient temperature. After washing, an anti-*Ng* rabbit IgG antibody (Fitzgerald Ind. catalog #20-NR08) diluted 1:500 in PBS was added for 2 hours at ambient temperature to label all the bacteria in the sample. Next, the coverslips were washed 3X with PBS, and incubated at ambient temperature for 1 hour with a goat anti-chicken-Alexa Fluor488 (Invitrogen catalog #A-11039) (diluted at 1:300), a goat anti-rabbit IgG, Alexa Fluor647 (Invitrogen catalog #A21244) (diluted at 1:1000), the actin probe phalloidin-Alexa Fluor555 (Invitrogen catalog #A30106) (diluted at 1:2000), and Hoechst (Invitrogen catalog #H3570) (diluted at 1:2000). After washing, coverslips were mounted on glass slides with ProLong Gold antifade reagent (Invitrogen catalog #P36984) and were examined by fluorescence microscopy. All images were acquired with an inverted wide-field microscope (Nikon Eclipse Ti) controlled by NES Elements v4.3 imaging software (Nikon) using a 60X/1.40 oil objective (Nikon Plan Apo λ), LED illumination (Lumencor) and CoolSNAP MYO CCD camera. Image acquisition and analysis were completed with NES Elements v4.3 imaging software. Actin recruitment at *Ng* colonies was quantified as before (Ivanov et al., 2021).

RNA extraction and quantitative real-time PCR

The RNA extraction and quantitative real-time PCR (qPCR) were performed as previously described (Ivanov et al., 2021). RNA was extracted from U937 M0 macrophages or M1 and M2 polarized macrophages using the RNeasy kit from Qiagen. First-strand cDNA synthesis was performed using TaqMan Gene Expression Cells-To-Ct kit (ThermoFisher catalog: AM1728). Relative mRNA levels were determined by quantitative real-time PCR using PowerUp SYBR Green master mix (ThermoFisher). For PowerUp SYBR Green, the thermal cycling was performed under the following conditions: pre-amplification: 95°C for 10min; amplification: 40 cycles at 95°C for 10s, 60°C for 10s, and 72°C for 10s; melting: 95°C for 10s, 60°C for 60s, and 97°C for 1s. Relative quantification was performed using $2^{-\Delta\Delta CT}$ method. Gene expression was normalized to *GAPDH* as a reference gene. A list of primers used in this study is presented in Supplementary Table 1.

Western blot analysis

U937 macrophages in M0, M1, and M2 polarization states were lysed in RIPA buffer prior to SDS-PAGE analysis and immunoblotting. Anti-FMNL2/3 (ab57963) mouse monoclonal antibody recognizing both FMNL2 and FMNL3 (Kage et al., 2017) was purchased from Abcam. Anti-actin (sc8432) mouse antibody was purchased from Santa Cruz.

Statistical analysis

Calculations for statistical differences were completed by Student's T-test or multiparametric ANOVA analysis using GraphPad Prism v10 software and data are presented in the respective figures' panels.

Results

Generation of bioluminescent *Ng* strain for bacterial growth analysis

Bioluminescence has emerged as a reliable approach for quantitative analysis of bacterial growth under various conditions, including in cellular infections (Waidmann et al., 2011; Brodl et al., 2018). Measurements of light output from bioluminescent bacteria allow growth kinetics analysis in a high-throughput manner with great resolution (Ondari et al., 2023). Because light production requires ATP, bioluminescence also reflects the metabolic state and viability of the producers (Gregor et al., 2018). We engineered a bioluminescent *Ng* FA1090 strain (*Ng* FA1090-LuxR) by inserting the LuxR operon (*luxCDABE*) from *Photorhabdus luminescens* on the *Ng* chromosome in the intergenic region of the *iga-trpB* locus (Ramsey et al., 2012) under the constitutive promoter of the gonococcal *opaB* gene using allelic exchange (Figure 1A). The *Ng iga-trpB* locus has been used frequently for chromosomal complementation studies because insertion of genetic elements does not affect bacterial replication (Ramsey et al., 2012). The bioluminescence output by the *Ng* FA1090-LuxR strain at various densities correlated well with alternative quantitative methods – namely, colony forming unit (CFU) counts (Figure 1B) and optical density measurement (Figure 1C) - with a linear dynamic range of at least two orders of magnitude (Figures 1B, C). The light output per CFU was similar (~ 0.15 RLUs/CFU) across several population densities (Figure 1D). In axenic liquid growth cultures with GCBL media (Kellogg et al., 1963), the parental FA1090 and FA1090-LuxR grew similarly indicating that bioluminescence production did not increase the metabolic burden sufficiently to affect bacterial replication (Figure 1E). The bioluminescence output of the FA1090-LuxR strain increased exponentially during logarithmic growth phase, peaked in the early stationary phase, and subsequently decreased (Figure 1F). Altogether, these results demonstrate that FA1090-LuxR grows with kinetics similar to the parental strain and bioluminescence production is an excellent readout in quantitative bacterial growth assays.

Neisseria gonorrhoeae grows in both nutrient-rich and nutrient-depleted conditions in the presence of human macrophages

We measured the growth of the FA1090-LuxR strain in macrophages infections using bioluminescence as a readout (Figures 2A, B). To this end, human U937 macrophages (Figure 2A) or primary monocyte-derived macrophages (hMDMs) (Figure 2B) were infected with FA1090-LuxR for 12 hrs in nutrients-depleted PBSG (PBS + 7.5 mM glucose) medium and bioluminescence output was measured hourly. In the absence of host cells, *Ng* does not grow in

10.3389/fcimb.2024.1384611

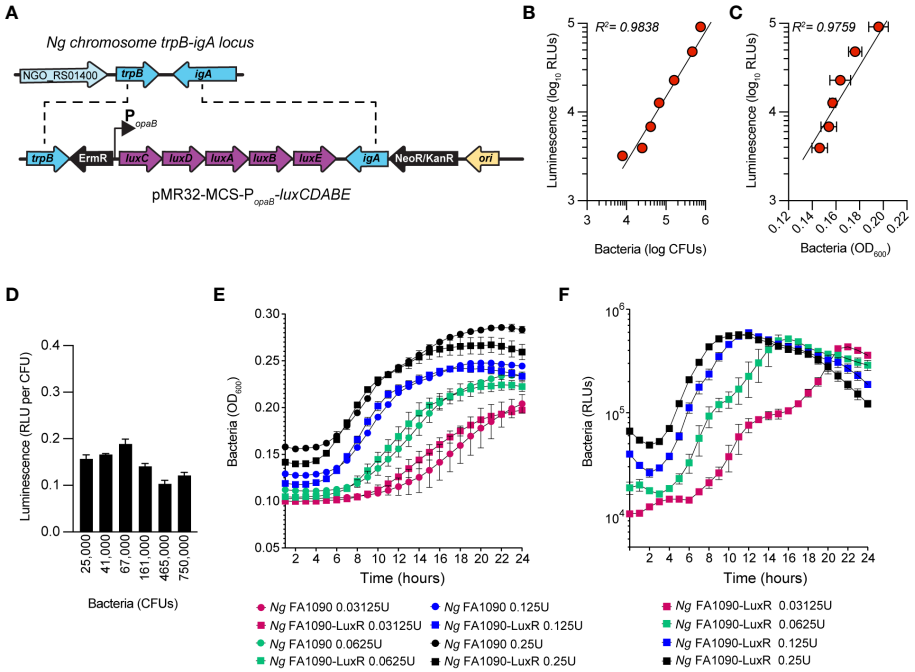

FIGURE 1
Construction and characterization of *Ng* FA1090-LuxR strain. **(A)** Construction of erythromycin-resistant FA1090-LuxR *Ng* strain via allelic exchange with pMR32-MCS-*luxCDABE* containing the LuxR operon cloned downstream of the constitutive *opaB* promoter (P_{opaB}). **(B, C)** Correlation between bioluminescence output (Luminescence RLUs) and bacterial population as measured by CFUs **(B)** or by optical density **(C)** for serial dilutions prepared from bacteria grown on GCB plates overnight. **(D)** Bioluminescence output per CFU is stable across several bacterial population densities. **(E, F)** Bacterial growth in axenic cultures with GCBL medium for several serial dilutions of *Ng* FA1090-LuxR and its parental strain over the indicated time period as measured by optical density (OD_{600}) **(E)** and luminescence output **(F)**. **(B–E)** Data is presented as an average from technical triplicates ± StDev, from one of three biological replicates.

PBSG medium (Chateau and Seifert, 2016; Ivanov et al., 2021) as evidenced by the progressive decline in the bioluminescence signal (Figure 2C). Conversely, the bioluminescence signal increases two orders of magnitude within 8 hrs post-infection (hpi) in PBSG medium when either U937 macrophages or hMDMs were present, indicative of explosive *Ng* replication (Figures 2A, B). Infections in nutrients replete RPMI medium slightly but statistically significantly enhanced *Ng* replication over the PBSG medium (Figures 2A, B); moreover, RPMI medium supported limited *Ng* replication even in the absence of host cells (Figure 2C) (Chateau and Seifert, 2016). Thus, macrophages can support robust *Ng* growth regardless of the nutrient abundance in the extracellular milieu. Next, *Ng* growth in macrophage infections was carried out in RPMI medium containing heat-inactivated human serum, which further increases nutrients abundance in the extracellular environment and is more relevant to human infection conditions. The addition of human serum reduced slightly the bacterial growth in U937 macrophages infections (Figure 2A). However, the addition of serum notably affected *Ng* growth in hMDM infections (Figure 2B). Together these data indicate that the presence of host cells rather than the nutritional content of the extracellular milieu is the important factor for *Ng* replication under infection conditions. Moreover, heat-inactivated human serum restricted *Ng* growth in RPMI medium in the absence of host cells (Figure 2C), suggestive of microbicidal activity. This serum-dependent growth restriction phenotype was more evident in hMDMs (Figure 2B) but not in U937 macrophages infections (Figure 2A) possibly due to invasion kinetics differences in the two cell types (Ivanov et al., 2021).

Neisseria gonorrhoeae invasion and intracellular growth are not dependent on extracellular nutrients

Because *Ng* colonizes macrophages and can replicate intracellularly as well as on the cell surface, we investigated whether nutrients availability affects invasion or bacterial replication in either of the niches. To this end, the invasion of U937 macrophages by gonococcal colonies was measured for the first 8 hrs of infection. A statistically significant increase in macrophages invasion was observed when infections were carried out in serum-containing RPMI medium as compared to infections in PBSG (Figure 3A) indicating that one or more factors in serum may directly or indirectly trigger the invasion process. Macrophages invasion is mediated by subversion of the actin cytoskeleton as an extensive network of cortical actin filaments forms at the plasma membrane at the invasion site and surrounds the invading colony even after internalization is complete (Ivanov et al., 2021). In all tested conditions, intracellular colonies were enveloped by actin filaments indicating that mechanistically the invasion process is similar under all three infection settings (Figure 3B). However, we

10.3389/fcimb.2024.1384611

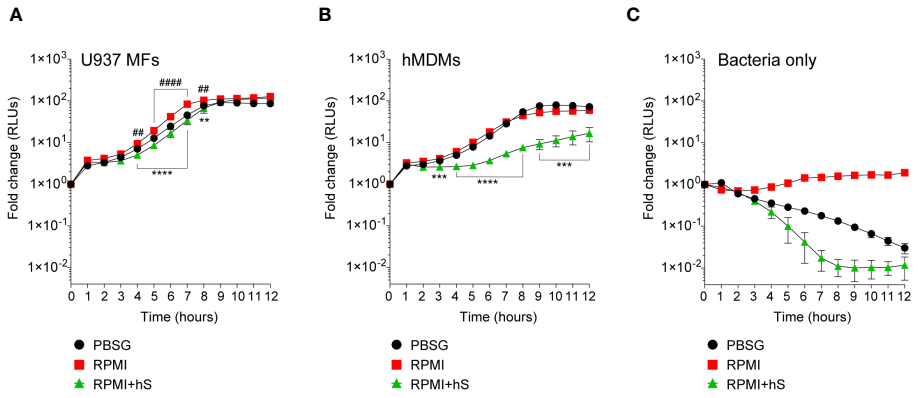

FIGURE 2
Kinetics of bacterial replication in the presence or absence of macrophages. **(A–C)** Quantitative analysis of FA1090-LuxR replication in the indicated media in the presence of either U937 macrophages (U937 MFs) **(A)** or primary human monocyte-derived macrophages (hMDMs) **(B)**, or in the absence of host cells (Bacteria only) **(C)**. Data is presented as fold change in bioluminescence (RLUs) from T0. Each time point is an average from six technical replicates ± StDev. Representative data from one of three biological replicates are shown. 'hS' – heat-inactivated human serum. Statistical differences were calculated using two-way ANOVA analysis and Dunnett method for multiple comparison test (*, statistical significance for RPMI *vs.* RPMI+hS; $^{\#}$, statistical significance for RPMI *vs.* PBSG. ** and $^{\#\#}$, $p < 0.01$; ***, $p < 0.001$; **** and $^{\#\#\#\#}$, $p < 0.0001$).

noted that when extracellular nutrients were present, the size of the intracellular colonies appeared larger as compared to PBSG conditions (Figure 3B). Therefore, intracellular replication was specifically measured by imaging and 3D volumetric size analysis in assays where colonies were allowed to invade U937 macrophages for 4 hrs and then expand intracellularly for additional 4 hrs (Figure 3C). Indeed, significant increase in the average colony size was observed in the presence of RPMI and RPMI+hS conditions. Thus, we conclude that nutrients-replete medium enhanced *Ng* intracellular replication in U937 macrophages and can enhance macrophage invasion when serum is present. Together, these data also indicate that the growth-promoting effect of the nutrients in the extracellular milieu is specific for bacteria replicating intracellularly because, in RPMI+hS *vs.* PBSG condition, the overall bacterial growth was lower (Figure 2A) but the intracellular growth was significantly enhanced (Figure 3C).

Macrophages in different immune activation states support Neisseria gonorrhoeae replication and invasion

To assess whether the phenotypic state of the macrophage impacts *Ng* capacity to colonize, invade, or replicate with it, U937 macrophages were polarized in pro-inflammatory M1-like state by stimulation with IFNγ and *E.coli* LPS, or in the tolerogenic M2-like state by treatment with IL-4 and IL-13 or were left in the M0 state (Nascimento et al., 2022). Successful polarization in the various phenotypic states was confirmed by the upregulation of state-specific cellular markers – *IRF1* and *IL6* for M1 and *IL10* for M2 (Figure 4A). Microbiocidal functions are enhanced in M1 macrophages (Thiriot et al., 2020), therefore we investigated whether M1-polarized U937 macrophages under the conditions we used restrict the replication of the vacuolar pathogen *Legionella pneumophila* as would be expected (Plumlee et al., 2009; Maciag et al., 2022). Indeed, M1-polarized U937 macrophages significantly restricted *Legionella* growth as compared to M0 controls (Figure 4B). However, M1-polarized U937 macrophages failed to restrict *Ng* growth irrespective of the cell culture media (PBSG, RPMI or RPMI+hS) used in the infection assays (Figures 4B, C). Importantly, the polarization phenotype of U937 macrophages did not change drastically after 8h of infection (Figure 4D), although we detected a statistically significant reduction (~30%) in *IRF1* expression, concomitant with a ~40% increase in *IL-10* in M1 polarized macrophages as compared to M0 controls. Overall, *IL10* levels were highest in M2 uninfected and infected macrophages as well as M0 infected macrophages.

Because IFNγ-dependent cell-autonomous defenses mainly target intracellular pathogens (Buchmeier and Schreiber, 1985; Nacy et al., 1985; Suzuki et al., 1988; Kak et al., 2018; Maciag et al., 2022), the lack of growth restriction by M1 macrophages might indicate that either intracellular gonococci can interfere with microbiocidal activities of M1 macrophages or perhaps enhanced replication by surface-associated bacteria compensates for a potential decrease in the intracellular population. To distinguish between those possibilities, we directly measured *Ng* capacity to invade and grow within M1 macrophages (Figures 5A–C). At 8 hpi, the number of gonococcal colonies inside M1 macrophages was reduced by ~40% for U937 cells (Figure 5A) and ~60% for hMDMs (Figure 5B), indicating that IFNγ-priming reduces invasion, or a fraction of intracellular colonies are eliminated. When we measured the expansion of gonococci intracellular colonies housed by the different macrophage types, the data revealed similar growth rates indicating that M1-polarized macrophages likely interfere with gonococcal invasion and not with intracellular replication (Figure 5C). Because the host actin nucleating factor FMNL3 mediates gonococcal invasion in macrophages (Ivanov et al., 2021), we compared the amount of *FMNL3* transcripts in polarized macrophages using qPCR analysis (Figure 5D) and protein expression using Western blot analysis (Figure 5E). *FMNL3* expression in M0 and M2 U937 cells was indistinguishable, however in M1 U937 cells the mRNA levels were reduced by 60%

10.3389/fcimb.2024.1384611

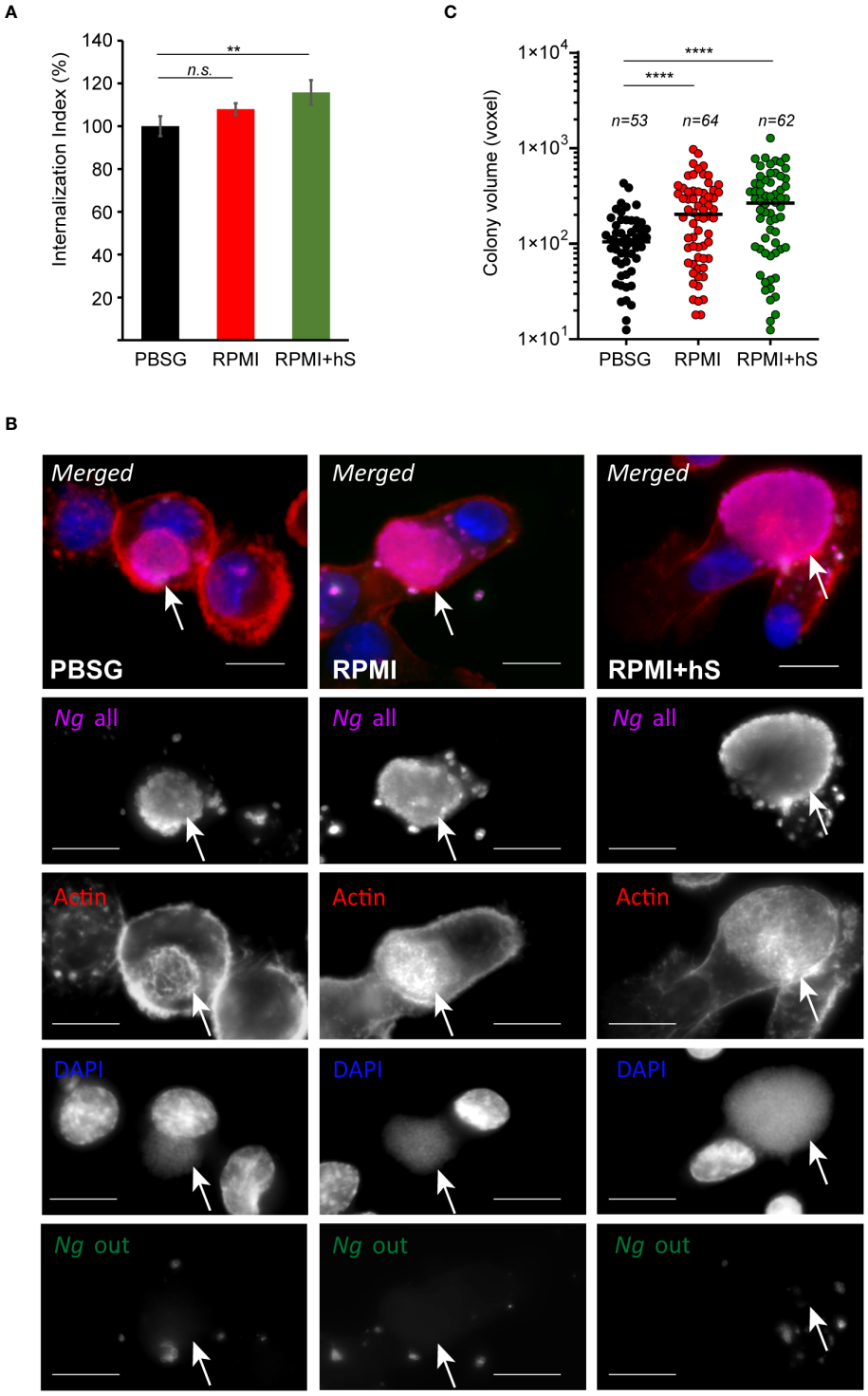

FIGURE 3
Extracellular nutrients abundance promotes gonococci invasion and intracellular growth in U937 macrophages. **(A)** Invasion of *Ng* colonies in macrophages cultured under nutrient-depleted (PBSG) and nutrient-replete conditions (RPMI and RPMI+hS) was determined at 8 hpi. The 'Internalization Index' reflects how each medium affects invasion compared to PBSG and was calculated for each condition by dividing the percentage of internalized microcolonies from the 'RPMI' and 'RPMI+hS' conditions by the percentage of internalized microcolonies from the 'PBSG' condition, which was then multiplied by 100. Graphs show averages of three biological replicates ± StDev. **(B)** Representative micrographs showing intracellular microcolonies at 8 hpi as determined by inside/out staining, where infections were carried out under nutrients-deplete (PBSG) or nutrients-replete (RPMI or RPMI+hS) conditions. Individual channels of the merged images are shown in grayscale. Arrows denote individual intracellular colonies. Bar = 10 µm. **(C)** Size measurements of individual intracellular colonies under the indicated growth conditions using 3D object volume microscopy measurements (in voxels). Each data point is derived from a single colony. The number of colonies included in the analysis is indicated for each condition. Means for each object population is shown. Representative data from one of three biological replicates are shown. **(A, C)** Statistical significance was determined via unpaired T-test analysis (*n.s.*, not significant; **, $p < 0.01$; ****, $p < 0.0001$).

10.3389/fcimb.2024.1384611

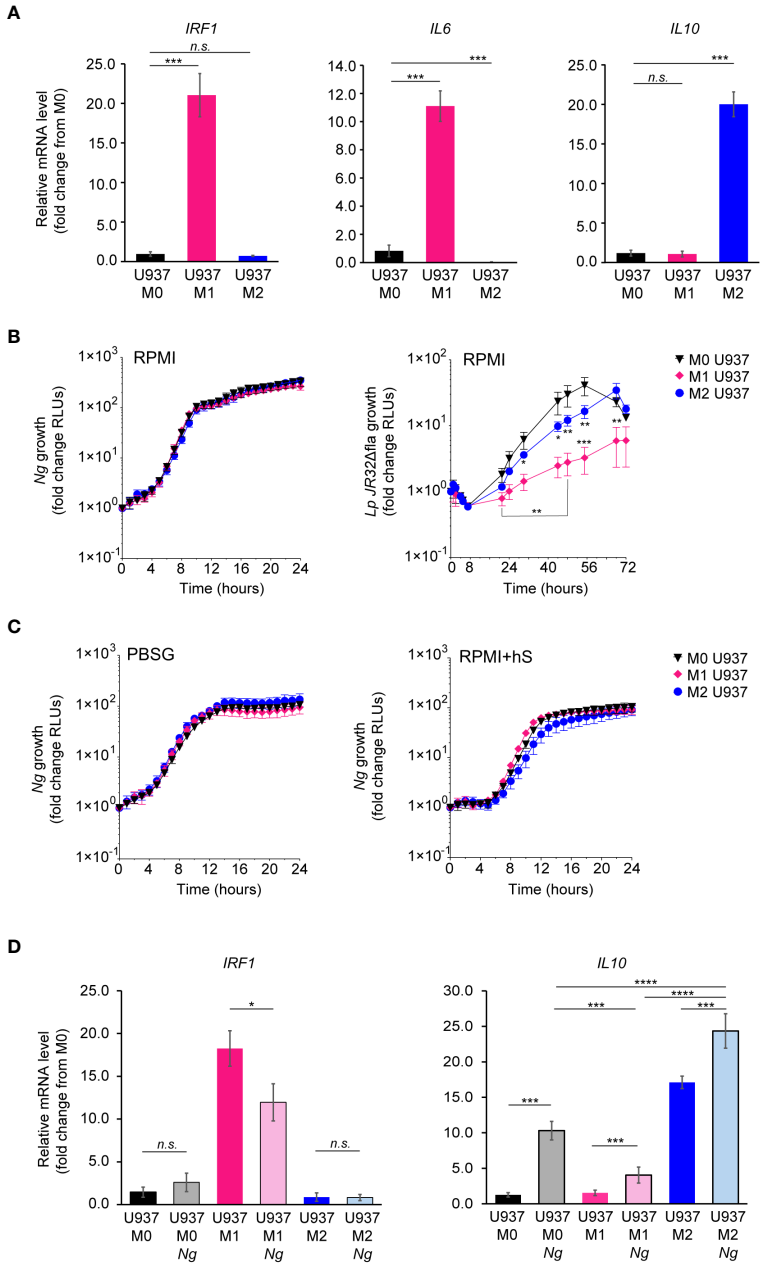

FIGURE 4
Kinetics of *Ng* replication with polarized U937 macrophages. **(A)** U937 macrophages polarization in M0, M1 and M2-like states was validated by qPCR analysis for expression of different markers associated with each phenotypic state – *IRF1* and *IL6* for M1 and *IL10* for M2. Graphs represent gene mRNA expression relative to M0 (fold change). **(B, C)** Kinetics of bacterial replication supported by M0, M1 and M2 macrophages under conditions of nutrient abundance or restriction. Growth is presented as fold change in bioluminescence for each condition from T_0. Data from *Ng* and *Lp* infections in RPMI are shown in **(B)** and data from *Ng* infections in PBSG or RPMI+hS are shown in **(C)**. **(D)** U937 macrophages polarization states in the presence and absence of *Ng* (8h infection) was determined by qPCR analysis for expression of different markers associated with each phenotypic state – *IRF1* for M1 and *IL10* for M2. Graphs represent gene mRNA expression relative to M0 (fold change). **(B, C)** Each data point on the graphs represents an average from technical triplicates ± StDev. Representative data from one of three biological replicates are shown. **(A, D)** Statistical significance was determined via unpaired T-test analysis (*n.s.*, not significant; *, $p < 0.05$; ***, $p < 0.001$; ****, $p < 0.0001$). **(B)** Statistical differences for M0 *vs.* M1 and M0 *vs.* M2 were calculated using two-way ANOVA analysis and Dunnett method for multiple comparison test (*, $p < 0.05$; **, $p < 0.01$; ***, $p < 0.001$).

(Figure 5D). This was also true for FMNL3 protein expression (Figure 5E). Even more, actin accumulation at *Ng* colonies was reduced in M1 macrophages (Figure 5F), consistent with a role for FMNL3 in actin polymerization at the site of invading colonies (Ivanov et al., 2021). Thus, M1-polarization results in the decrease of a host factor mediating gonococcal invasion, which potentially might explain the defect in M1 cells. If lowered FMNL3 expression in M1 reduced gonococcal invasion, it would be expected that overexpression of FMNL3 from a heterologous promoter should restore invasion in M1 macrophages. To this end, we used a pool of U937 macrophages in which ~50% of the cells stably overexpress V5-tagged FMNL3 from a CMV promoter to measure gonococcal

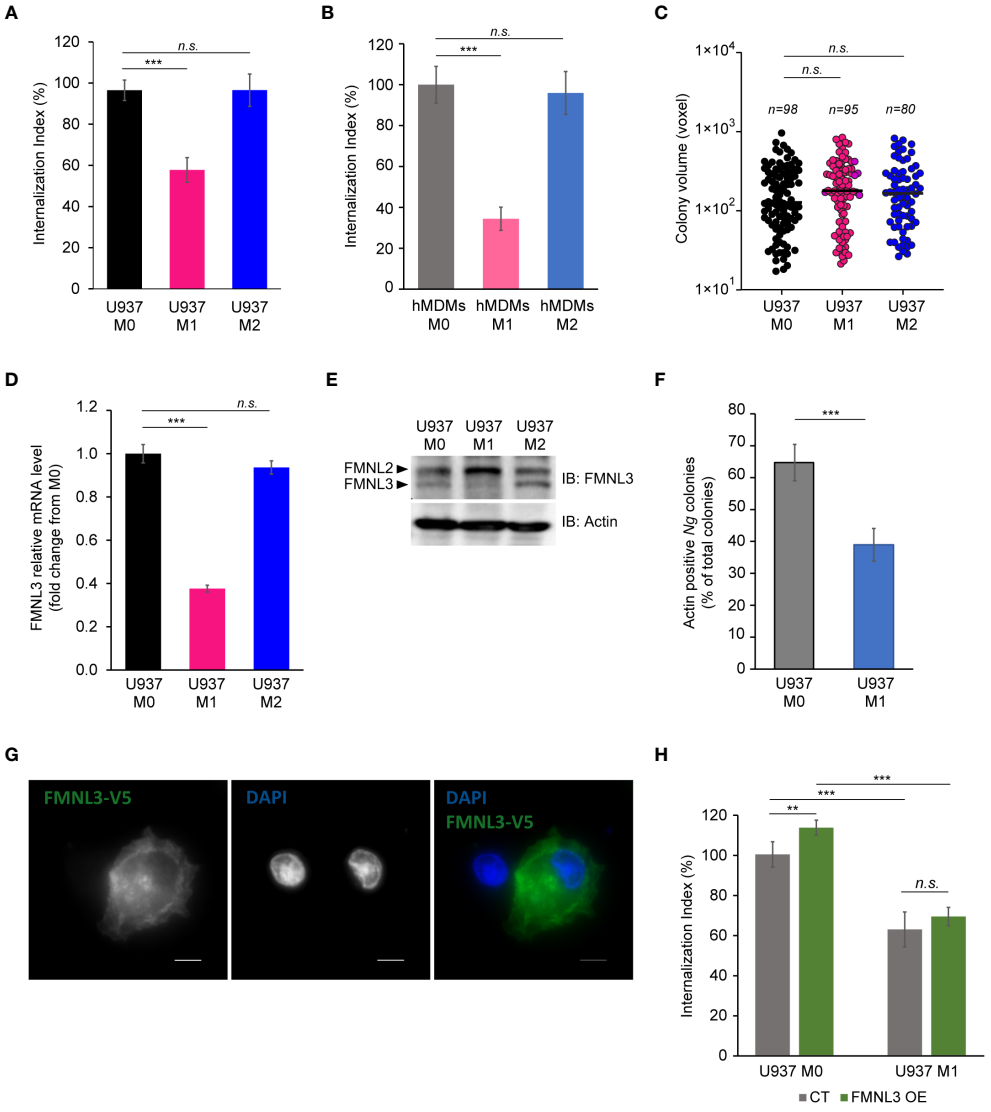

FIGURE 5
Ng invasion and intracellular replication in polarized macrophages. **(A, B)** Invasion of *Ng* colonies in polarized macrophages was determined at 8 hpi. The 'Internalization Index' reflects how each phenotypic state affects invasion compared to M0 and was calculated for each condition by dividing the percentage of internalized microcolonies from M1 and M2 conditions by the percentage of internalized microcolonies by M0 macrophages, which was then multiplied by 100. Data from infections of polarized U937 macrophages **(A)** and hMDMs **(B)** are shown. Graphed data represent averages of three biological replicates ± StDev. **(C)** The sizes of intracellular colonies harbored by polarized U937 macrophages as determined by 3D object volume microscopy measurements (in voxels). Each data point is derived from a single colony. The number of colonies included in the analysis is indicated for each condition. Representative data from one of three biological replicates are shown. **(D, E)** Gene expression analysis for *FMNL3* in polarized U937 macrophages as determined by qPCR **(D)** and protein expression as determined by Western blot with an FMNL3 antibody **(E)**. Graphed data represent *FMNL3* expression under different conditions relative to expression in M0 (fold change) **(D)**. **(F)** Actin recruitment at surface-associated, invading, and internalized *Ng* colonies was determined in U937 M0 and U937 M1 infected macrophages at 8hpi. The graph shows the percentage of actin-positive *Ng* colonies of total *Ng* colonies. Graphed data represent averages of three biological replicates ± StDev. **(G)** Representative micrograph showing FMNL3-V5 expression in a pool of U937 macrophages that either overexpress the allele (right cell) or not (left cell). Individual channels of the merged images are shown in grayscale. Bar = 5 µm. **(H)** Gonococcal invasion of a heterogenous pool of M0 or M1 polarized U937 macrophages that either express FMNL3-V5 (OE) or not (CT). The 'Internalization Index' was calculated at 8 hpi and is normalized to the percentage of colonies internalized by M0 CT cells, which was set at 100%. Graphs show averages of three biological replicates ± StDev. **(A-D, F, H)** Statistical analyses were completed by unpaired Student's T-test (*n.s.*, not significant; **, $p < 0.01$; ***, $p < 0.001$).

invasion (Ivanov et al., 2021) (Figure 5G). However, *Ng* invasion was equally reduced under M1-polarizing conditions regardless of whether macrophages overexpressed FMNL3-V5 or not (Figure 5H), indicating that lower FMNL3 expression alone does not account for the invasion blockade. The FMNL3-V5 allele is functional and has previously complemented the invasion defect observed in FMNL3 KO macrophages (Ivanov et al., 2021). Thus, we conclude that: (i) M1-polarization reduces *FMNL3* expression and blocks gonococcal invasion by a mechanism that cannot be overcome by restoration of FMNL3 abundance; (ii) macrophages support robust intracellular as well as extracellular gonococcal replication regardless of the phenotypic polarization state and the availability of extracellular nutrients; (iii) increased replication of surface-associated bacteria likely compensates for the decreased intracellular bacterial

population brought by the invasion blockade under M1-polarization conditions. Taken together, our data demonstrate that gonococci have evolved mechanisms to colonize successfully and replicate in association with macrophages regardless of their polarization state.

Discussion

Lack of protective immunity against reinfection represents one notable aspect of gonococcal infections that hampers vaccine development. The weakened immunological response is a result of extensive host adaptation and the development of multiple innate and adaptive immunosuppressive mechanisms (Liu et al., 2011; Russell et al., 2019; Russell et al., 2020). The subversion of mucosal macrophages – the tissue sentinels in the genitourinary tract (Givan et al., 1997; Pudney et al., 2005) – into putative cellular niches and immunoregulators in gonococcal infections is noted as an important knowledge gap (Russell et al., 2019; Russell et al., 2020). Once gonococci cross the urogenital epithelium and invade the submucosal space, the bacteria gain access to tissue-resident as well as monocytes-derived macrophages recruited to the infection site. Previous studies showed that gonococci can promote an M2-like polarization state in human macrophages which is incapable of inducing CD4+ T cell proliferation (Ortiz et al., 2015). Gonococci elicit the production of pro- as well as anti-inflammatory cytokines when cultured with macrophages *in vitro*. However, IL10 secretion was induced at much lower bacterial loads as compared to IL6 (Ortiz et al., 2015), indicating potential skewing towards a more anti-inflammatory response, which is consistent with the prevalent asymptomatic nature of the infection. Here we investigated whether and to what extent macrophage polarization affects the cell capacity to function as a niche for bacterial replication. When gonococci colonize macrophages, bacterial replication takes place either in a surface-associated or within an internalized microcolony (Ivanov et al., 2021). Despite potent microbiocidal capacity towards intracellular bacteria, our data demonstrates that M1 macrophages could not restrict *Ng* growth but did reduce invasion. These observations indicate that *Ng* replication likely takes place preferentially in surface-associated colonies because of reduction in the number of intracellular microcolonies. These data further support our original premise that dual niche occupancy enhances evasion of cell-autonomous host defenses (Ivanov et al., 2021). Moreover, gonococci intracellular replication in M1 and M0 macrophages was indistinguishable despite a robust restriction of *Legionella* intracellular replication after M1 polarization. This phenotype provides strong evidence for the existence of *Ng*-encoded mechanisms directed towards the evasion of microbiocidal activities of M1 macrophages. The unique membrane-bound organelle harboring the intracellular gonococcal colony does not fuse with lysosomes and lacks endosomal markers (Ivanov et al., 2021), and our data demonstrates that even under M1 polarization conditions the vacuole protects the bacteria from host microbiocidal activities. Disruption of pathogen-occupied vacuoles by IFNγ-inducible gene products can trigger cytosolic cell-autonomous defense responses that culminate in either host cell death or autophagolysosomal clearance (MacMicking, 2012; Meunier and Broz, 2016; Kak et al., 2018). However, we did not observe signs of either in M1 macrophages invaded by *Ng* (data not shown) indicating that the vacuolar compartment is intact and supported bacterial replication. Gonococci have been shown to interfere with apoptotic responses, thus a blockade of IFNγ-dependent host cell death response may also play a role for intracellular survival in M1 macrophages. We also investigated if infection with *Ng* changes macrophages polarization. Indeed, we observed a reduction in *IFR1* expression in M1 macrophages infected with *Ng* for 8h (Figure 4D). While we noticed a slight increase in *IL10* induction after infection in M1 macrophages, overall gene expression suggests that *Ng* does not reprogram M1 macrophages in M2 during the 8h infection we used in our experimental set-up. Whether prolonged infection changes the phenotype of M1 macrophages remains to be determined. The immune evasion mechanisms facilitating intracellular replication in M1 macrophages thus warrant further investigation. It is notable that under all polarization conditions tested, gonococci replication rates intracellularly and overall (intracellularly + extracellularly) were comparable, indicating that *Ng* is well adapted to exploit macrophages for growth regardless of their polarization state. This was not the case for *Legionella* – an accidental human pathogen – which could not overcome the antimicrobial defenses of M1 macrophages.

Our data demonstrated that M1 polarization reduced invasion but not intracellular replication. Notably, stimulation with IFNγ/LPS decreased expression of FMNL3 – an actin nucleator from the formin family that mediates actin polymerization necessary for gonococcal invasion (Ivanov et al., 2021). As a result, actin accumulation at *Ng* colonies was also reduced in M1 macrophages. Overexpression of FMNL3 under heterologous promoter, however, did not increase invasion in M1 macrophages; therefore, other regulators upstream or downstream of FMNL3 are also affected as a result of M1 polarization. Indeed, we have shown that multiple formins or myosin motors could regulate gonococcal invasion (Ivanov et al., 2021).

The present study also investigated the impact of extracellular nutrients on gonococcal replication with macrophages. In the absence of macrophages, limited gonococcal growth is observed in nutrient-replete medium (RPMI), whereas nutrient-depleted (PBSG) medium did not support gonococcal replication (Figure 2B) (Chateau and Seifert, 2016; Ivanov et al., 2021). When either primary or immortalized macrophages were present, the gonococci population overall increased 2 orders of magnitude within 8 hpi regardless of the culture media used in the assays. Notably, when heat-inactivated human serum was provided, gonococcal growth with hMDMs was delayed and reduced as compared to serum-free infections, indicating that a serum-associated activity either directly or indirectly might interfere with gonococcal growth. Given that in all our experimental conditions we use heat-inactivated human serum during infection, we suspect that the presence of anti-microbial peptides rather than complement is responsible for the growth phenotype. Direct interference with bacterial replication by human serum was also observed in the absence of macrophages. Moreover, intracellular gonococci were protected from the anti-microbial activity of the human serum in macrophage infections and intracellular growth

increased under those conditions. Gonococci invade U937 macrophages faster as compared to hMDMs (Ivanov et al., 2021), thus the number of intracellular bacteria as a percentage of the total population is also higher, which explains why the bactericidal effect of human serum, which targets surface-associated and extracellular bacteria, is pronounced in hMDM infections. The increase in intracellular growth likely compensates partially for the decrease in extracellular replication when serum is present, and we also observed increased invasion when human serum was present in the culture media. Collectively, our data demonstrates intracellular gonococci replication is primarily affected by the nutrient content of the extracellular milieu, whereas intracellular growth occurred under all conditions but was significantly enhanced when nutrients were present.

Data availability statement

The original contributions presented in the study are included in the article/Supplementary Material. Further inquiries can be directed to the corresponding author/s.

Author contributions

MJ: Conceptualization, Data curation, Formal analysis, Investigation, Methodology, Validation, Writing – original draft, Writing – review & editing. MM: Investigation, Methodology, Validation, Writing – original draft, Writing – review & editing. RY: Investigation, Validation, Writing – original draft, Writing – review & editing. ND: Investigation, Validation, Writing – original draft, Writing – review & editing. AT: Investigation, Validation, Writing – original draft, Writing – review & editing. SI: Conceptualization, Data curation, Formal analysis, Funding acquisition, Methodology, Writing – original draft, Writing – review & editing. A-MD: Conceptualization, Data curation, Formal analysis, Funding acquisition, Investigation, Methodology, Project administration, Supervision, Validation, Writing – original draft, Writing – review & editing.

Funding

The author(s) declare financial support was received for the research, authorship, and/or publication of this article. This work was supported by grants from the following funding sources: NIGMS (P20GM134974-5749) to AMD and NIAID (AI143839) to SI.

Conflict of interest

The authors declare that the research was conducted in the absence of any commercial or financial relationships that could be construed as a potential conflict of interest.

Publisher's note

Supplementary material

The Supplementary Material for this article can be found online at: https://www.frontiersin.org/articles/10.3389/fcimb.2024.1384611/full#supplementary-material

References

Almeida, L., Dhillon-LaBrooy, A., and Sparwasser, T. (2023). The evolutionary tug-of-war of macrophage metabolism during bacterial infection. *Trends Endocrinol. Metab.*35(3):235–248. doi: 10.1016/j.tem.2023.11.002

Atri, C., Guerfali, F. Z., and Laouini, D. (2018). Role of human macrophage polarization in inflammation during infectious diseases. *Int. J. Mol. Sci.* 19(6):1801. doi: 10.3390/ijms19061801

Bah, A., and Vergne, I. (2017). Macrophage autophagy and bacterial infections. *Front. Immunol.* 8, 1483. doi: 10.3389/fimmu.2017.01483

Barrientos-Durán, A., Fuentes-López, A., de Salazar, A., Plaza-Díaz, J., and García, F. (2020). Reviewing the composition of vaginal microbiota: inclusion of nutrition and probiotic factors in the maintenance of eubiosis. *Nutrients* 12(2):419. doi: 10.3390/nu12020419

Brodl, E., Niederhauser, J., and Macheroux, P. (2018). *In situ* measurement and correlation of cell density and light emission of bioluminescent bacteria. *J. Vis. Exp.* 136:57881. doi: 10.3791/57881

Buchmeier, N. A., and Schreiber, R. D. (1985). Requirement of endogenous interferon-gamma production for resolution of Listeria monocytogenes infection. *Proc. Natl. Acad. Sci. United States America.* 82, 7404–7408. doi: 10.1073/pnas.82.21.7404

Chateau, A., and Seifert, H. S. (2016). Neisseria gonorrhoeae survives within and modulates apoptosis and inflammatory cytokine production of human macrophages. *Cell. Microbiol.* 18, 546–560. doi: 10.1111/cmi.v18.4

Criss, A. K., Katz, B. Z., and Seifert, H. S. (2009). Resistance of Neisseria gonorrhoeae to non-oxidative killing by adherent human polymorphonuclear leucocytes. *Cell. Microbiol.* 11, 1074–1087. doi: 10.1111/cmi.2009.11.issue-7

Criss, A. K., and Seifert, H. S. (2008). Neisseria gonorrhoeae suppresses the oxidative burst of human polymorphonuclear leukocytes. *Cell. Microbiol.* 10, 2257–2270. doi: 10.1111/cmi.2008.10.issue-11

Criss, A. K., and Seifert, H. S. (2012). A bacterial siren song: intimate interactions between Neisseria and neutrophils. *Nat. Rev. Microbiol.* 10, 178–190. doi: 10.1038/nrmicro2713

Dilworth, J. A., Hendley, J. O., and Mandell, G. L. (1975). Attachment and ingestion of gonococci human neutrophils. *Infection immunity.* 11, 512–516. doi: 10.1128/iai.11.3.512-516.1975

Dong, Q., Nelson, D. E., Toh, E., Diao, L., Gao, X., Fortenberry, J. D., et al. (2011). The microbial communities in male first catch urine are highly similar to those in paired urethral swab specimens. *PloS One* 6, e19709. doi: 10.1371/journal.pone.0019709

Dunkelberger, J. R., and Song, W. C. (2010). Complement and its role in innate and adaptive immune responses. *Cell Res.* 20, 34–50. doi: 10.1038/cr.2009.139

Dwivedy, A., and Aich, P. (2011). Importance of innate mucosal immunity and the promises it holds. *Int. J. Gen. Med.* 4, 299–311. doi: 10.2147/IJGM.S17525

Escobar, A., Candia, E., Reyes-Cerpa, S., Villegas-Valdes, B., Neira, T., Lopez, M., et al. (2013). Neisseria gonorrhoeae induces a tolerogenic phenotype in macrophages to modulate host immunity. *Mediators inflammation.* 2013, 127017. doi: 10.1155/2013/127017

Escobar, A., Rodas, P. I., and Acuña-Castillo, C. (2018). Macrophage-neisseria gonorrhoeae interactions: A better understanding of pathogen mechanisms of immunomodulation. *Front. Immunol.* 9, 3044. doi: 10.3389/fimmu.2018.03044

Feeley, J. C., Gibson, R. J., Gorman, G. W., Langford, N. C., Rasheed, J. K., Mackel, D. C., et al. (1979). Charcoal-yeast extract agar: primary isolation medium for Legionella pneumophila. *J. Clin. Microbiol.* 10, 437–441. doi: 10.1128/jcm.10.4.437-441.1979

Givan, A. L., White, H. D., Stern, J. E., Colby, E., Gosselin, E. J., Guyre, P. M., et al. (1997). Flow cytometric analysis of leukocytes in the human female reproductive tract: comparison of fallopian tube, uterus, cervix, and vagina. *Am. J. Reprod. Immunol.* 38, 350–359. doi: 10.1111/j.1600-0897.1997.tb00311.x

Gregor, C., Gwosch, K. C., Sahl, S. J., and Hell, S. W. (2018). Strongly enhanced bacterial bioluminescence with the ilux operon for single-cell imaging. *Proc. Natl. Acad. Sci. United States America.* 115, 962–967. doi: 10.1073/pnas.1715946115

Grobeisen-Duque, O., Mora-Vargas, C. D., Aguilera-Arreola, M. G., and Helguera-Repetto, A. C. (2023). Cycle biodynamics of women's microbiome in the urinary and reproductive systems. *J. Clin. Med.* 12(12):4003. doi: 10.3390/jcm12124003

Gunderson, C. W., and Seifert, H. S. (2015). Neisseria gonorrhoeae elicits extracellular traps in primary neutrophil culture while suppressing the oxidative burst. *MBio* 6(1):e02452-14. doi: 10.1128/mBio.02452-14

Hook, E. W. 3rd (1987). Gonococcal infections: a continuing diagnostic and therapeutic challenge. *Md Med. J.* 36, 48–53.

Imarai, M., Candia, E., Rodriguez-Tirado, C., Tognarelli, J., Pardo, M., Perez, T., et al. (2008). Regulatory T cells are locally induced during intravaginal infection of mice with Neisseria gonorrhoeae. *Infection immunity.* 76, 5456–5465. doi: 10.1128/IAI.00552-08

Ivanov, S. S., Castore, R., Juarez Rodriguez, M. D., Circu, M., and Dragoi, A. M. (2021). Neisseria gonorrhoeae subverts formin-dependent actin polymerization to colonize human macrophages. *PloS pathogens.* 17, e1010184. doi: 10.1371/journal.ppat.1010184

Jorgensen, I., Rayamajhi, M., and Miao, E. A. (2017). Programmed cell death as a defence against infection. *Nat. Rev. Immunol.* 17, 151–164. doi: 10.1038/nri.2016.147

Kage, F., Winterhoff, M., Dimchev, V., Mueller, J., Thalheim, T., Freise, A., et al. (2017). FMNL formins boost lamellipodial force generation. *Nat. Commun.* 8, 14832. doi: 10.1038/ncomms14832

Kak, G., Raza, M., and Tiwari, B. K. (2018). Interferon-gamma (IFN-γ): Exploring its implications in infectious diseases. *Biomol Concepts.* 9, 64–79. doi: 10.1515/bmc-2018-0007

Kellogg, D. S.Jr., Peacock, W. L.Jr., Deacon, W. E., Brown, L., and Pirkle, D. I. (1963). NEISSERIA GONORRHOEAE. I. VIRULENCE GENETICALLY LINKED TO CLONAL VARIATION. *J. bacteriology.* 85, 1274–1279. doi: 10.1128/jb.85.6.1274-1279.1963

Krakauer, T. (2019). Inflammasomes, autophagy, and cell death: the trinity of innate host defense against intracellular bacteria. *Mediators inflammation.* 2019, 2471215. doi: 10.1155/2019/2471215

Lenz, J. D., and Dillard, J. P. (2018). Pathogenesis of neisseria gonorrhoeae and the host defense in ascending infections of human fallopian tube. *Front. Immunol.* 9, 2710. doi: 10.3389/fimmu.2018.02710

Liu, Y., Feinen, B., and Russell, M. W. (2011). New concepts in immunity to Neisseria gonorrhoeae: innate responses and suppression of adaptive immunity favor the pathogen, not the host. *Front. Microbiol.* 2, 52. doi: 10.3389/fmicb.2011.00052

Locati, M., Curtale, G., and Mantovani, A. (2020). Diversity, mechanisms, and significance of macrophage plasticity. *Annu. Rev. Pathol.* 15, 123–147. doi: 10.1146/annurev-pathmechdis-012418-012718

Maciag, K., Raychowdhury, R., Smith, K., Schneider, A. M., Coers, J., Mumbach, M. R., et al. (2022). IRF3 inhibits IFN-γ-mediated restriction of intracellular pathogens in macrophages independently of IFNAR. *J. leukocyte Biol.* 112, 257–271. doi: 10.1002/JLB.3A0218-069RR

MacMicking, J. D. (2012). Interferon-inducible effector mechanisms in cell-autonomous immunity. *Nat. Rev. Immunol.* 12, 367–382. doi: 10.1038/nri3210

Martinez, F. O., Helming, L., and Gordon, S. (2009). Alternative activation of macrophages: an immunologic functional perspective. *Annu. Rev. Immunol.* 27, 451–483. doi: 10.1146/annurev.immunol.021908.132532

McGee, Z. A., Johnson, A. P., and Taylor-Robinson, D. (1981). Pathogenic mechanisms of Neisseria gonorrhoeae: observations on damage to human fallopian tubes in organ culture by gonococci of colony type 1 or type 4. *J. Infect. diseases.* 143, 413–422. doi: 10.1093/infdis/143.3.413

Meunier, E., and Broz, P. (2016). Interferon-inducible GTPases in cell autonomous and innate immunity. *Cell. Microbiol.* 18, 168–180. doi: 10.1111/cmi.12546

Nacy, C. A., Fortier, A. H., Meltzer, M. S., Buchmeier, N. A., and Schreiber, R. D. (1985). Macrophage activation to kill Leishmania major: activation of macrophages for intracellular destruction of amastigotes can be induced by both recombinant interferon-gamma and non-interferon lymphokines. *J. Immunol.* 135, 3505–3511. doi: 10.4049/jimmunol.135.5.3505

Nascimento, C. R., Rodrigues Fernandes, N. A., Gonzalez Maldonado, L. A., and Rossa Junior, C. (2022). Comparison of monocytic cell lines U937 and THP-1 as macrophage models for *in vitro* studies. *Biochem. Biophys. Rep.* 32, 101383. doi: 10.1016/j.bbrep.2022.101383

Nelson, D. E., van der Pol, B., Dong, Q., Revanna, K. V., Fan, B., Easwaran, S., et al. (2010). Characteristic male urine microbiomes associate with asymptomatic sexually transmitted infection. *PloS One* 5, e14116. doi: 10.1371/journal.pone.0014116

Nobs, S. P., and Kopf, M. (2021). Tissue-resident macrophages: guardians of organ homeostasis. *Trends Immunol.* 42, 495–507. doi: 10.1016/j.it.2021.04.007

Ondari, E., Wilkins, A., Latimer, B., Dragoi, A. M., and Ivanov, S. S. (2023). Cellular cholesterol licenses Legionella pneumophila intracellular replication in macrophages. *Microb. Cell.* 10, 1–17. doi: 10.15698/mic

Ortiz, M. C., Lefimil, C., Rodas, P. I., Vernal, R., Lopez, M., Acuna-Castillo, C., et al. (2015). Neisseria gonorrhoeae modulates immunity by polarizing human macrophages to a M2 profile. *PloS One* 10, e0130713. doi: 10.1371/journal.pone.0130713

Palmer, A., and Criss, A. K. (2018). Gonococcal defenses against antimicrobial activities of neutrophils. *Trends Microbiol.* 26, 1022–1034. doi: 10.1016/j.tim.2018.07.003

Plumlee, C. R., Lee, C., Beg, A. A., Decker, T., Shuman, H. A., and Schindler, C. (2009). Interferons direct an effective innate response to Legionella pneumophila infection. *J. Biol. Chem.* 284, 30058–30066. doi: 10.1074/jbc.M109.018283

Pudney, J., Quayle, A. J., and Anderson, D. J. (2005). Immunological microenvironments in the human vagina and cervix: mediators of cellular immunity are concentrated in the cervical transformation zone. *Biol. reproduction.* 73, 1253–1263. doi: 10.1095/biolreprod.105.043133

Quillin, S. J., and Seifert, H. S. (2018). Neisseria gonorrhoeae host adaptation and pathogenesis. *Nat. Rev. Microbiol.* 16, 226–240. doi: 10.1038/nrmicro.2017.169

Ramsey, M. E., Hackett, K. T., Kotha, C., and Dillard, J. P. (2012). New complementation constructs for inducible and constitutive gene expression in Neisseria gonorrhoeae and Neisseria meningitidis. *Appl. Environ. Microbiol.* 78, 3068–3078. doi: 10.1128/AEM.07871-11

Rice, P. A., Shafer, W. M., Ram, S., and Jerse, A. E. (2017). Neisseria gonorrhoeae: drug resistance, mouse models, and vaccine development. *Annu. Rev. Microbiol.* 71, 665–686. doi: 10.1146/annurev-micro-090816-093530

Russell, M. W., Gray-Owen, S. D., and Jerse, A. E. (2020). Editorial: immunity to neisseria gonorrhoeae. *Front. Immunol.* 11, 1375. doi: 10.3389/fimmu.2020.01375

Russell, M. W., Jerse, A. E., and Gray-Owen, S. D. (2019). Progress toward a gonococcal vaccine: the way forward. *Front. Immunol.* 10, 2417. doi: 10.3389/fimmu.2019.02417

Shapouri-Moghaddam, A., Mohammadian, S., Vazini, H., Taghadosi, M., Esmaeili, S. A., Mardani, F., et al. (2018). Macrophage plasticity, polarization, and function in health and disease. *J. Cell Physiol.* 233, 6425–6440. doi: 10.1002/jcp.26429

Sica, A., and Mantovani, A. (2012). Macrophage plasticity and polarization: *in vivo* veritas. *J. Clin. Invest.* 122, 787–795. doi: 10.1172/JCI59643

Song, W., Condron, S., Mocca, B. T., Veit, S. J., Hill, D., Abbas, A., et al. (2008). Local and humoral immune responses against primary and repeat Neisseria gonorrhoeae genital tract infections of 17beta-estradiol-treated mice. *Vaccine* 26, 5741–5751. doi: 10.1016/j.vaccine.2008.08.020

Stevens, J. S., and Criss, A. K. (2018). Pathogenesis of Neisseria gonorrhoeae in the female reproductive tract: neutrophilic host response, sustained infection, and clinical sequelae. *Curr. Opin. hematology.* 25, 13–21. doi: 10.1097/MOH.0000000000000394

Suzuki, Y., Orellana, M. A., Schreiber, R. D., and Remington, J. S. (1988). Interferon-gamma: the major mediator of resistance against Toxoplasma gondii. *Sci. (New York NY).* 240, 516–518. doi: 10.1126/science.3128869

Thiriot, J. D., Martinez-Martinez, Y. B., Endsley, J. J., and Torres, A. G. (2020). Hacking the host: exploitation of macrophage polarization by intracellular bacterial pathogens. *Pathog. Dis.* 78(1):ftaa009. doi: 10.1093/femspd/ftaa009

Tuddenham, S., Ghanem, K. G., Caulfield, L. E., Rovner, A. J., Robinson, C., Shivakoti, R., et al. (2019). Associations between dietary micronutrient intake and molecular-Bacterial Vaginosis. *Reprod. Health* 16, 151. doi: 10.1186/s12978-019-0814-6

Unemo, M., Golparian, D., Sanchez-Buso, L., Grad, Y., Jacobsson, S., Ohnishi, M., et al. (2016). The novel 2016 WHO Neisseria gonorrhoeae reference strains for global quality assurance of laboratory investigations: phenotypic, genetic and reference genome characterization. *J. Antimicrob. Chemother.* 71, 3096–3108. doi: 10.1093/jac/dkw288

Unemo, M., Lahra, M. M., Escher, M., Eremin, S., Cole, M. J., Galarza, P., et al. (2021). WHO global antimicrobial resistance surveillance for Neisseria gonorrhoeae 2017-18: a retrospective observational study. *Lancet Microbe* 2, e627–ee36. doi: 10.1016/S2666-5247(21)00171-3

Waidmann, M. S., Bleichrodt, F. S., Laslo, T., and Riedel, C. U. (2011). Bacterial luciferase reporters: the Swiss army knife of molecular biology. *Bioeng Bugs.* 2, 8–16. doi: 10.4161/bbug.2.1.13566